

# Review

## Electrical applications of carbon materials

D. D. L. CHUNG

*Composite Materials Research Laboratory, University at Buffalo, The State University of New York, Buffalo, NY 14260-4400, USA*

The electrical applications of carbons and their composites are reviewed, with emphasis on applications that are relevant to industrial needs. The applications include electrical conduction, electrical contacts, electrodes, electromagnetic interference shielding, resistance heating, thermoelectricity, sensing, electrical switching, electronic devices and thermal pastes. The carbons include graphite, coke, carbon fibers, carbon filaments, carbon black and flexible graphite. © 2004 Kluwer Academic Publishers

### 1. Introduction

Carbon materials (including composite materials containing carbon) are well-known for their structural applications, which relate to aerospace structures, aircraft brakes, concrete structures and lubrication. They are also known for their thermal applications (which relate to heat conduction and thermal insulation), environmental applications (which involve activated carbon) and biomedical applications (which pertain to implants). Less well-known are the electrical applications, though the electronic properties have long been studied for the purpose of fundamental understanding of the physics of carbons. This review is focused on the electrical applications, particularly those that are relevant to industrial needs. These applications include electrical conduction, electrodes, electromagnetic reflection, heating, thermal conduction, thermoelectricity, sensing, electrical switching and electronic devices.

### 2. Electrical conduction

Due to the in-plane delocalization of the  $p_z$  electrons, carbon is an electrical conductor in the in-plane direction. However, the out-of-plane conductivity is low, due to the van der Waals bonding in this direction. Therefore, the electrical conductivity of a carbon material depends greatly on the degree of preferred orientation of the carbon layers. This degree is enhanced by heat treatment, high graphitizability of the precursor materials and alignment of the carbon units (such as the carbon fibers in a composite material) during processing. As a result, carbon materials exhibit a wide range of electrical conductivity, thereby allowing a variety of electrical conduction applications, as described below.

Petroleum coke is a low-cost and plentiful form of carbon. Compared to graphite, it is less crystalline and thus less conductive. However, due to its lower crystallinity, it is less prone to shear and is thus superior in mechanical strength.

### 2.1. Electrically conductive additive in an electrochemical electrode

Due to the fact that some electrochemical electrode materials are not conductive electrically, a conductive additive is added to the electrochemically active species in forming the electrode [1–6]. An example is manganese dioxide ( $\text{MnO}_2$ ), which is not conducting and serves as the cathode of various electrochemical cells, including lithium cells. Due to the chemically inert and electrically conductive nature of carbons, carbons are used as the conductive additive. Among the carbons, carbon black is particularly common for this purpose.

Other than the electrochemically active materials and the conductive additive, the electrode contains a binder, which is commonly a thermoplastic polymer, such as polytetrafluoroethylene (PTFE, or teflon) and polyvinylidene fluoride (PVDF) in the form of particles. The binder, upon heating, serves to bind the ingredients together to form a shaped object (such as a disc) that can be handled. The type and amount of binder are expected to affect not only the bindability, but also the distribution of the carbon additive.

Carbon black is more effective than 0.1  $\mu\text{m}$ -diameter carbon filament (catalytically grown from methane, referred to in this paper as carbon filament [7]) without graphitization as a conductive additive for the  $\text{MnO}_2$  cathode [8], even though a carbon black compact without  $\text{MnO}_2$  exhibits higher resistivity than a carbon filament compact without  $\text{MnO}_2$  [9]. Thus, a low resistivity for a carbon compact does not imply a low resistivity for an  $\text{MnO}_2$ -carbon composite. This is because the resistivity of an  $\text{MnO}_2$ -carbon composite depends on the dispersion and connectivity of the carbon in the midst of  $\text{MnO}_2$  particles. In spite of the large aspect ratio of the carbon filament, the carbon black is superior as a conductive additive, because of the spreadability of carbon black between the  $\text{MnO}_2$  particles [8].

Table I [9] gives the resistivity and density of the ten different compositions of the  $\text{MnO}_2$  cathode. At a binder content of 10 wt%, graphitized carbon filament and graphitized mesophase pitch (both graphitized at

TABLE I The basic characteristics of various types of carbon

	C (%)	$d_{002}$ (Å)	BET specific surface area (m <sup>2</sup> /g)	Particle size (μm)
Graphitized mesophase pitch	99.90	3.369	5.23	12
Natural graphite	99.89	3.362	2.75	27
Graphitized carbon filament	99.70	3.360	26.4	/
Carbon filament	99.70	3.367	53.9	/
Carbon black <sup>a</sup>	/	/	2.8	0.05

<sup>a</sup>Pore size = 18.9 Å.

2800°C) give the lowest resistivity, while carbon filament without graphitization gives the highest resistivity. The resistivity of the cathode containing natural graphite is quite low, in spite of the low density. The cathode containing graphitized carbon filament exhibits lower resistivity than that containing graphitized mesophase pitch, in spite of the lower density of the former. At a binder content of 6 wt%, carbon black and graphitized carbon filament give the lowest resistivity, while natural graphite and graphitized mesophase pitch give the highest resistivity.

At either binder content, graphitization of the carbon filament decreases the resistivity of the MnO<sub>2</sub> cathode, while increasing the density slightly. At either binder content, carbon black gives a cathode of lower resistivity than carbon filament without graphitization, as mentioned above.

For all the types of carbon except carbon black, decrease in binder content increases the resistivity. For all the types of carbon, a decrease in binder content increases the density slightly. Thus, except for carbon black, the resistivity increases in spite of an increase in density. This effect is attributed to the decrease in the degree of dispersion of the carbon as the binder content decreases. In other words, the binder helps the dispersion of the carbon, except for carbon black, the dispersion of which relates to the spreadability of the carbon black between the MnO<sub>2</sub> particles. In contrast, the other types of carbon cannot spread upon squeezing and, so, their dispersion needs the help of the binder more.

A decrease in binder content from 10 to 6 wt% increases the resistivity of cathodes with carbon filaments (whether graphitized or not), but not drastically. On the other hand, the resistivity increases drastically upon decreasing the binder content for the cases of graphitized mesophase pitch and natural graphite. This means that particulate carbon requires the help of the binder for its dispersion more severely than filamentous carbon. This is reasonable, since the large aspect ratio of filamentous carbon enhances connectivity and hence decreases the importance of dispersion.

Among the ten compositions in Table I, the cathode containing 10 wt% binder and graphitized carbon filament gives the lowest resistivity. However, the cathode containing 10 wt% binder and graphitized mesophase pitch gives almost as low a resistivity, and graphitized mesophase pitch is less expensive than graphitized carbon filament. On the other hand, the low density of

the cathode containing graphitized carbon filament is attractive for electrochemical cells with a high energy density. For a low density, natural graphite is even more attractive, though the resistivity is higher. In general, the choice of a carbon type in practice depends on the resistivity, density and cost.

The use of carbon filament in place of carbon black as the conductive additive in an Li/MnO<sub>2</sub> primary cell causes the running voltage near cell end-of-life to decline gradually, in contrast to the abrupt end-of-life when carbon black is used. The gradualness toward end-of-life is due to a high electron transfer rate and a high rate of electrolyte absorption. In order for the filaments to be effective, they need to undergo solvent cleansing prior to use [8].

## 2.2. Current collector, electrical contact and electrode

Current collectors are used in electrochemical cells (batteries and fuel cells). Electrical contacts are needed in electrical measurements and in the application of a current or voltage for the purpose of cathodic protection (corrosion protection). Both current collectors and electrical contacts require materials that are electrically conducting. In the case of current collectors in electrochemical cells, chemical resistance is also required.

Carbon does not have an oxide on it, whereas metals tend to have an oxide coating. As the oxide is relatively poor in electrical conductivity, a metal conductor tends to degrade with time in air. The absence of an oxide makes carbon attractive, even though carbon is not as conductive as metals.

Carbon filament is superior to carbon black in lithium primary cells which use carbon as a porous electrode (current collector) [10]. The current collector of the lithium/thionyl chloride (Li/SOCl<sub>2</sub>) cell conventionally uses carbon black, which needs a teflon binder. The removal of the hydrocarbon layer on the carbon filament improves the electrochemical behavior, as indicated by the electron transfer rate across the electrode-electrolyte interface [11]. Due to the cleansing ability of thionyl chloride (the catholyte), carbon filament used in place of carbon black does not require solvent cleansing prior to use. As the filaments tend to cling together, a binder is not necessary, in contrast to carbon black. Using the same paper-making process, the carbon filament can be made into a thinner sheet than carbon black. The thinness is valuable for enhancing the energy density (particularly the specific gravimetric energy density) of the cell, as the area over which the lithium anode faces the carbon current collector is increased. In addition, the packing density is lower for the filament sheet than the carbon black sheet, so that the catholyte absorptivity is higher for the filament sheet than the carbon black and consequently the energy density is further increased [9].

A fuel cell is a galvanic cell in which the reactants for the anodic and cathodic reactions are continuously being supplied. In the most common type of fuel cell, the hydrogen-oxygen fuel cell, hydrogen gas is the reactant for the anodic reaction and oxygen is the reactant for the cathodic reaction and H<sub>2</sub>O is the overall reaction

product. The reactions need a catalyst (typically platinum), which is applied on a porous carbon that serves as the current collector. There are two current collectors, one for the anode side and one for the cathode side. The cathodic reaction produces  $\text{OH}^-$  ions, which move from the cathode side to the anode side, where they combine with hydrogen to provide the anodic reaction. Electrons produced by the anodic reaction are collected by the current collector at the anode side. They move through the outer circuit and enter the current collector at the cathode side, where the electrons are consumed to provide the cathodic reaction. The product of the overall reaction is  $\text{H}_2\text{O}$  (steam) which comes out from the bottom of the cell. Between the two current collectors is the electrolyte. Carbon black, submicron carbon filament and other carbons are used as the current collector material. A comparative study of the effectiveness of these carbons is still needed.

Electrical contacts are commonly applied in the form of a paste. Fine graphite flakes dispersed in water to form a colloid, with the presence of small amounts of a binder (such as polyvinyl alcohol) and a dispersing agent, are commonly used as an electrical contact material. Though the conductivity is lower than that attained by using silver particles in place of graphite flakes, the cost is much lower than the silver particle counterpart. Short carbon fibers are not suitable for this application, due to the high viscosity and poor screen-printability resulted from the fibers.

Another application that is akin to that of an electrical contact is the use of graphite as an electrode material in electrostatic discharge machining (EDM). This application requires low electrical resistivity, high hardness, and high flexural and compressive strengths. These properties are attained by using fine-grained isotropic graphite of resistivity  $10^{-3} \Omega\cdot\text{cm}$ .

Isotropic graphite, after copper metal impregnation, exhibits resistivity  $10^{-4} \Omega\cdot\text{cm}$ . The impregnated form is a composite material which is particularly useful for sliding electrical contacts or brushes, as needed for motors, generators, commutators, alternators and electric trams.

The graphite or coke rods used as electrodes (anodes) in an electrolytic cell for producing aluminum from aluminum oxide by the Hall-Heroult process also serve as electrical contacts [12]. The graphite or coke is gradually consumed by oxidation to form  $\text{CO}_2$ , while  $\text{Al}_2\text{O}_3$  (dissolved in  $\text{Na}_3\text{AlF}_6$ ) is reduced to Al.

In the case of cement-based electrical contacts, which are needed for cathodic protection of the steel reinforcing bars in concrete, short carbon fibers are effective. Cathodic protection is one of the most common and effective methods for corrosion control of steel reinforced concrete. This method involves the application of a voltage so as to force electrons to go to the steel reinforcing bar (rebar), thereby making the steel a cathode. For directing electrons to the steel reinforced concrete to be cathodically protected, an electrical contact is needed on the concrete. The electrical contact is electrically connected to the voltage supply. One of the choices of an electrical contact material is zinc, which is a coating deposited on the concrete by thermal spraying. It

has a very low volume resistivity (thus requiring no metal mesh embedment), but it suffers from poor wear and corrosion resistance, the tendency to oxidize, high thermal expansion coefficient, and high material and processing costs. Another choice is a conductor filled polymer [13], which can be applied as a coating without heating, but it suffers from poor wear resistance, high thermal expansion coefficient and high material cost. Yet another choice is a metal (e.g., titanium) strip or wire embedded at one end in cement mortar, which is in the form of a coating on the steel reinforced concrete. The use of carbon fiber mortar [14], coke powder mortar [15–17] or coke powder asphalt [18–21] for this coating facilitates cathodic protection, as it is advantageous to enhance the conductivity of this coating. Due to the decrease in resistivity associated with carbon fiber addition (1.1 vol%) to mortar, overlay (embedding titanium wires for electrical contacts to steel reinforced concrete) in the form of mortar containing carbon fiber and latex reduces by 10% the driving voltage required for cathodic protection, compared to plain mortar overlay [14]. In spite of the low resistivity of mortar overlay with carbon fiber, cathodic protection requires multiple metal electrical contacts embedded in the mortar at a spacing of 11 cm or less [14].

### 2.3. Controlled electrical resistivity materials

Controlled electrical resistivity materials are used for controlled electrical conduction, static charge dissipation and lightning protection in electronic, mechanical, structural, chemical and vacuum applications. These materials are typically in the form of composite materials with an electrically insulating matrix and an electrically conductive discontinuous filler, which can be particulate or fibrous. The higher is the filler content, the lower is the resistivity of the composite. These composites include those with polymer [22–25], ceramic [26–30] and cement [31] matrices. Polymers and ceramics are usually insulating electrically, but cement is slightly conductive. Polymers that are electrically conductive exist, but they are expensive. Among all these matrices, cement is the least expensive. In addition, the fabrication of cement-matrix composites is inexpensive and takes place at room temperature. The fabrication of ceramic-matrix composites such as alumina-matrix composites is even more expensive than that of polymer-matrix composites, due to the high processing temperatures. Furthermore, cement-matrix composites, like ceramic-matrix composites, are mechanically more rugged and chemically more resistant than polymer-matrix composites.

In addition to providing a range of electrical resistivity, controlled resistivity materials provide a range of dielectric constant. As the filler content of a ceramic-matrix composite increases, the dielectric constant increases and the resistivity decreases [26]. In the case of an alumina-matrix  $\text{TiO}_2$  particulate composite, the relative dielectric constant (1 kHz) is 127,000 (undesirably high) when the resistivity is  $5 \times 10^5 \Omega\cdot\text{cm}$  and the  $\text{Al}_2\text{O}_3$  content is >80 wt%; the relative dielectric constant

(1 kHz) is 26.6 when the resistivity is  $1 \times 10^9 \Omega\text{-cm}$  and the  $\text{Al}_2\text{O}_3$  content is  $>94 \text{ wt\%}$  [26]. It would be desirable to have the combination of low resistivity (for charge dissipation and related functions) and low dielectric constant (to avoid a capacitive effect). Polymer matrices tend to exhibit lower values of dielectric constant than ceramic or cement matrices, but they tend to be insufficient for mechanical ruggedness and chemical and temperature resistance.

The combination of low resistivity, low dielectric constant, mechanical ruggedness and low cost is provided by using cement-matrix composites containing electrically conductive short fibers such as carbon fiber and steel fiber. With carbon fiber (1.0 vol%) and silica fume, the resistivity is  $8 \times 10^2 \Omega\text{-cm}$  and the relative dielectric constant is 49 [31]. The fiber also improves the mechanical properties and decreases the drying shrinkage [32].

### 3. Electromagnetic reflection

Carbon is a good reflector of electromagnetic radiation. The reflection is valuable for electromagnetic interference (EMI) shielding and for guiding an electromagnetic wave. The relevant radiation is in the radio wave and microwave regimes.

EMI shielding refers to the reflection and/or absorption of electromagnetic radiation by a material, which thereby acts as a shield against the penetration of the radiation through the shield. As electromagnetic radiation, particularly that at high frequencies (e.g., radio waves, such as those emanating from cellular phones) tend to interfere with electronics (e.g., computers), EMI shielding of both electronics and radiation source is needed and is increasingly required by governments around the world. The importance of EMI shielding relates to the high demand of today's society on the reliability of electronics and the rapid growth of radio frequency radiation sources [33, 34]. EMI shielding is to be distinguished from magnetic shielding, which refers to the shielding of magnetic fields at low frequencies (e.g., 60 Hz). Materials for EMI shielding are different from those for magnetic fielding.

The primary mechanism of EMI shielding is usually reflection. For reflection of the radiation by the shield, the shield must have mobile charge carriers (electrons or holes) which interact with the electromagnetic fields in the radiation. As a result, the shield tends to be electrically conducting, although a high conductivity is not required. For example, a volume resistivity of the order of  $1 \Omega\text{-cm}$  is typically sufficient. However, electrical conductivity is not the scientific criterion for shielding, as conduction requires connectivity in the conduction path (percolation in case of a composite material containing a conductive filler), whereas shielding does not. Although shielding does not require connectivity, it is enhanced by connectivity. Metals are by far the most common materials for EMI shielding. They function mainly by reflection due to the free electrons in them. Metal sheets are bulky, so metal coatings made by electroplating, electroless plating or vacuum deposition are commonly used for shielding [35–38]. The coating may be on bulk materials, fibers or particles.

Coatings tend to suffer from their poor wear or scratch resistance.

### 3.1. Carbon composites

Due to the skin effect, a composite material having a conductive filler with a small unit size of the filler is more effective than one having a conductive filler with a large unit size of the filler. For effective use of the entire cross-section of a filler unit for shielding, the unit size of the filler should be comparable to or less than the skin depth. Therefore, a filler of unit size  $1 \mu\text{m}$  or less is typically preferred, though such a small unit size is not commonly available for most fillers and the dispersion of the filler is more difficult when the filler unit size decreases. Metal coated polymer fibers or particles are used as fillers for shielding, but they suffer from the fact that the polymer interior of each fiber or particle does not contribute to shielding.

Polymer-matrix composites containing conductive fillers are attractive for shielding [39–44] due to their processability (e.g., moldability), which helps to reduce or eliminate the seams in the housing that is the shield. The seams are commonly encountered in the case of metal sheets as the shield and they tend to cause leakage of the radiation and diminish the effectiveness of the shield. In addition, polymer-matrix composites are attractive in their low density. The polymer matrix is commonly electrically insulating and does not contribute to shielding, though the polymer matrix can affect the connectivity of the conductive filler and connectivity enhances the shielding effectiveness. In addition, the polymer matrix affects the processability.

Electrically conducting polymers [45–48] are becoming increasingly available, but they are not common and tend to be poor in the processability and mechanical properties. Nevertheless, electrically conducting polymers do not require a conductive filler in order to provide shielding, so that they may be used with or without a filler. In the presence of a conductive filler, an electrically conducting polymer matrix has the added advantage of being able to electrically connect the filler units that do not touch one another, thereby enhancing the connectivity.

Cement is slightly conducting, so the use of a cement matrix also allows the conductive filler units in the composite to be electrically connected, even when the filler units do not touch one another. Thus, cement-matrix composites have higher shielding effectiveness than corresponding polymer-matrix composites in which the polymer matrix is insulating [49]. Moreover, cement is less expensive than polymers and cement-matrix composites are useful for the shielding of rooms in a building [50–52]. Similarly, carbon is a superior matrix than polymers for shielding due to its conductivity, but carbon-matrix composites are expensive [53].

Due to the electrical conductivity and chemical resistance of carbons, carbons are suitable for use as an electrically conductive filler in composite materials. EMI shielding is one of the main applications of conventional short carbon fibers [54]. Due to the small diameter and the skin effect, carbon filaments (catalytically grown, of diameter  $0.1 \mu\text{m}$ ) are more effective at the

same volume fraction in a composite than conventional short carbon fibers for EMI shielding, as shown for both thermoplastic [55, 56] and cement [57, 58] matrices. In this paper, filaments refer to those of diameter less than 1  $\mu\text{m}$ , whereas fibers refer to those of diameter 1  $\mu\text{m}$  or more. In a thermoplastic matrix, carbon filaments at 19 vol% give an EMI shielding effectiveness of 74 dB at 1 GHz [56], whereas carbon fibers (isotropic pitch based, 3000  $\mu\text{m}$  long) at 20 vol% give a shielding effectiveness of 46 dB at 1 GHz [55]. In a cement-matrix composite, fiber volume fractions are typically less than 1%. Carbon filaments at 0.54 vol% in a cement paste give an effectiveness of 26 dB at 1.5 GHz [57], whereas carbon fibers (isotropic pitch based, 3 mm long) at 0.84 vol% in a mortar give an effectiveness of 15 dB at 1.5 GHz [58]. The highest few values of EMI shielding effectiveness reported in cement-matrix composites are (i) 40 dB, as attained in cement paste containing 1.5 vol% carbon filaments [59], (ii) 49 dB, as attained in cement paste containing 1.0 vol% coke powder [60], and (iii) 70 dB, as attained in cement paste containing 0.72 vol% stainless steel fibers of diameter 8  $\mu\text{m}$  and length 6 mm [61].

### 3.2. Colloidal carbon

Colloidal graphite is fine graphite powder suspended in a liquid carrier (such as water and alcohol), together with a small amount of a polymeric binder. After application of colloidal graphite on a surface by painting or other methods, the liquid carrier evaporates, thus allowing the graphite particles to be essentially in direct contact. The resulting coating is effective for electromagnetic interference (EMI) shielding [62–64]. It is commonly used for shielding in television scopes. However, research on colloidal graphite has mostly focused on the performance as a lubricant [65, 66].

Colloidal graphite conventionally uses submicron graphite particles. However, the use of 0.1  $\mu\text{m}$ -diameter carbon filaments is attractive for shielding [65] due to the small diameter and large aspect ratio. The small diameter is advantageous for formation of a stable colloid and for shielding (due to the skin effect). The large aspect ratio is advantageous for shielding and for enhancing the toughness of the resulting coating.

The EMI shielding effectiveness of colloidal graphite is improved by the combined use of graphite particles and 0.1  $\mu\text{m}$  diameter discontinuous carbon filaments [65]. The addition of 30 wt% carbon filaments to a commercial graphite colloid increases the shielding effectiveness from 11 to 20 dB for a water-based graphite colloid with a starch-type binder, and from 24 to 38 dB for a water-based graphite colloid without binder.

A colloid may be used as an admixture in cement, in addition to being used as a coating on various materials. Due to the hydraulic nature of cement, a water-based colloid is suitable. A water-based colloid of submicron graphite particles is an effective admixture for enhancing the EMI shielding effectiveness of cement paste, though it is ineffective for lowering the electrical resistivity [66]. As an admixture, it is more effective for shielding than 15  $\mu\text{m}$  diameter carbon fibers, though it is less effective than 0.1  $\mu\text{m}$  diameter carbon filaments.

A shielding effectiveness of 22 dB at 1 GHz is reached by cement paste at a solid graphite content of 0.92 vol%, compared to a value of 11 dB for a coating made from the graphite colloid and a value of 14 dB for graphite colloid coated cement paste (without admixture).

### 3.3. Flexible graphite

A seam in a housing that serves as an EMI shield needs to be filled with an EMI gasket (i.e., a resilient EMI shielding material), which is commonly a material based on an elastomer, such as rubber and silicone [67–70]. An elastomer is resilient, but is itself not able to shield, unless it is coated with a conductor (e.g., a metal coating called metallization) or is filled with a conductive filler (typically metal particles such as Ag-Cu). The coating suffers from its poor wear resistance due to the tendency for the coating to debond from the elastomer. The use of a conductive filler suffers from the resulting decrease in resilience, especially at a high filler volume fraction that is usually required for sufficient shielding effectiveness. As the decrease in resilience becomes more severe as the filler concentration increases, the use of a filler that is effective even at a low volume fraction is desirable. Therefore, the development of EMI gaskets is more challenging than that of EMI shielding materials in general.

For a general EMI shielding material in the form of a composite material, a filler that is effective at a low concentration is also desirable, although it is not as critical as for EMI gaskets. This is because the strength and ductibility of a composite tend to decrease with increasing filler content when the filler-matrix bonding is poor. Poor bonding is quite common for thermoplastic polymer matrices. Furthermore, a low filler content is desirable due to the greater processability, which decreases with increasing viscosity. In addition, a low filler content is desirable due to the cost saving and weight saving.

In order for a conductive filler to be highly effective, it preferably should have a small unit size (due to the skin effect), a high conductivity (for shielding by reflection and absorption) and a high aspect ratio (for connectivity). Metals are more attractive for shielding than carbons due to their higher conductivity, though carbons are attractive in their oxidation resistance and thermal stability. Fibers are more attractive than particles due to their high aspect ratio. Thus, metal fibers of a small diameter are desirable. Nickel filament of diameter 0.4  $\mu\text{m}$  (as made by electroplating carbon filament of diameter 0.1  $\mu\text{m}$ ) is particularly effective [70–72]. Nickel is more attractive than copper due to its superior oxidation resistance. The oxide film is poor in conductivity and is thus detrimental to the connectivity among filler units.

Continuous fiber polymer-matrix structural composites that are capable of EMI shielding are needed for aircrafts and electronic enclosures [53, 73–77]. The fibers in these composites are typically carbon fibers, which may be coated with a metal (e.g., nickel [78]) or be intercalated (i.e., doped) to increase the conductivity [79, 80]. An alternate design involves the use of glass fibers (not conducting) and conducting interlayers in

the composite [81, 82]. Yet another design involves the use of activated carbon fibers, the moderately high specific surface area (90 m<sup>2</sup>/g) of which results in extensive multiple reflections while the tensile properties are maintained [83].

A particularly attractive EMI gasket material is flexible graphite, which is a flexible sheet made by compressing a collection of exfoliated graphite flakes (called worms) without a binder. During exfoliation, an intercalated graphite (graphite compound with foreign species called the intercalate between some of the graphite layers) flake expands typically by over 100 times along the *c*-axis. Compression of the resulting worms (like accordions) causes the worms to be mechanically interlocked to one another, so that a sheet is formed without a binder.

Due to the exfoliation, flexible graphite has a large specific surface area (e.g., 15 m<sup>2</sup>/g). Due to the absence of a binder, flexible graphite is essentially entirely graphite (other than the residual amount of intercalate in the exfoliated graphite). As a result, flexible graphite is chemically and thermally resistant, and low in coefficient of thermal expansion (CTE). Due to its microstructure involving graphite layers that are preferentially parallel to the surface of the sheet, flexible graphite is high in electrical and thermal conductivities in the plane of the sheet. Due to the graphite layers being somewhat connected perpendicular to the sheet (i.e., the honeycomb microstructure of exfoliated graphite), flexible graphite is electrically and thermally conductive in the direction perpendicular to the sheet (although not as conductive as the plane of the sheet). These in-plane and out-of-plane microstructures result in resilience, which is important for EMI gaskets. Due to the skin effect, a high surface is desirable for shielding. As the electrical conductivity (especially that in the plane of the sheet) and specific surface area are both quite high in flexible graphite, the effectiveness of this material for shielding is exceptionally high (up to 130 dB at 1 GHz) [84].

#### 4. Resistance heating

Electrical heating includes resistance heating (i.e., Joule heating) and induction heating, in addition to heating by the use of electric heat pumps, plasmas and lasers [85, 86]. It is to be distinguished from solar heating [87–91] and the use of fossil fuels such as coal, fuel oil and natural gas [86]. Due to the environmental problem associated with the use of fossil fuels and due to the high cost of solar heating, electrical heating is increasingly important.

Resistance heating involves passing an electric current through a resistor, which is the heating element. In relation to the heating of a structure, resistance heating typically involves the embedding of a heating element in the structure or attaching a heating element on the structure. The materials of heating elements cannot be too low in electrical resistivity, as this would result in the resistance of the heating element being too low. The materials of heating elements cannot be too high in resistivity either, as this would result in the current in the heating element being too low (unless the voltage is very high). Materials of heating elements include

metal alloys (such as nichrome), ceramics (such as silicon carbide [92]), graphite [93, 94], polymer-matrix composites [95–97], carbon-carbon composites [98], asphalt [99] and concrete [100].

Resistance heating is useful for industrial processes, the heating of buildings, the deicing of bridge decks [101] and aircraft [95], and the demolition of concrete structures [102, 103].

A less common form of resistance heating involves eddy current heating which accompanies induction heating [104]. However, the requirement of induction heating makes this form of resistance heating relatively expensive.

#### 4.1. Flexible graphite

Graphite has long been used as a heating element. In addition to graphite in a monolithic form [93], pyrolytic graphite deposited on boron nitride has been used [105]. Furthermore, polymer-matrix composites containing carbon fibers [106] or carbon black [107], cement-matrix composites containing coke powder [108–110] and carbon-matrix composites [98, 111] have been used. Flexibility or shape conformability of the heating element is desirable for many applications, such as the deicing of aircraft [112, 113] and the heating of floors, pipes and boilers. Flexible graphite is thus attractive [114, 115]. It is also attractive because it is in a sheet form, is corrosion-resistant, does not need to be encased and does not need machining for shaping. In contrast, conventional graphite requires expensive machining to attain the shape required for the heating element. Flexible graphite provides temperatures up to 980°C (though burn-off occurs in air at 980°C), response half-time down to 4 s, and heat output at 60 s up to 5600 J [116]. The electrical energy for heating by 1°C is 1–2 J in the initial portion of rapid temperature rise. The temperature and heat output increase with decreasing thickness of the flexible graphite sheet.

#### 4.2. Carbon fiber mats

Due to their flexibility, carbon fiber mats (porous mats consisting of short carbon fibers and a small amount of an organic binder) are attractive for use as heating elements. In addition, they are attractive because they are in a sheet form, corrosion resistant, and can be incorporated in a structural composite.

A mat comprising bare short carbon fibers and exhibiting volume electrical resistivity of 0.11 Ω·cm and thermal stability up to 205°C has been found to be an effective resistive heating element [117]. It provides temperatures up to 134°C at a power of up to 6.5 W, with a time up to 106 s to reach half of the maximum temperature rise. The electrical energy input to heat by 1°C during the initial period of rapid temperature rise (5 s) was up to 3.8 J. The time to drop to half of the maximum temperature rise during cooling is much longer than the time to reach half of the maximum temperature during heating, especially when the input power is low. A mat comprising Ni/Cu/Ni coated carbon fibers gives lower temperatures, due to the lower resistance, but it gives faster response.

Flexible graphite is superior to carbon fiber mats as a heating element, as it provides much higher temperatures and much faster response.

## 5. Thermoelectric energy conversion

Thermoelectric behavior pertains to the conversion between thermal and electrical energy. In particular, the Seebeck effect is a thermoelectric effect in which a voltage results from a temperature gradient, which causes the movement of charge carriers from the hot point to the cold point. This voltage (Seebeck voltage) is useful for temperature sensing and pertains also to the generation of electrical energy. The negative of the change in Seebeck voltage (hot minus cold) per degree C in temperature rise (hot minus cold) is called the thermoelectric power, the thermopower, or the Seebeck coefficient.

Electrical energy generation involves the Seebeck effect, in which a temperature gradient gives rise to a voltage between the hot and cold ends. Heating and cooling involve the Peltier effect, in which heat is evolved (i.e., heating) or absorbed (i.e., cooling) upon passage of an electric current across two dissimilar materials that are electrically connected. The Seebeck effect provides a renewable source of energy, in addition to providing the basis for thermocouples, which are used for temperature measurement. Moreover, it is relevant to the reduction of environmental pollution and global warming. The Peltier effect is relevant to air conditioning, refrigeration and thermal management.

The Peltier effect requires a combination of low thermal conductivity, high electrical conductivity and high thermoelectric power. Due to their high thermal conductivity, carbons are not suitable for the Peltier effect. Therefore, this section is focused on the Seebeck effect. The Seebeck effect at cryogenic temperatures has long been studied in various carbons for the purpose of understanding the electronic properties, but this section emphasizes the carbon forms that are relevant to thermoelectric applications at temperatures at or above room temperature. These forms include carbon fiber composites and flexible graphite. The former is attractive due to its use in structures. The latter is attractive due to its compliance, which is needed for the coupling between a thermoelectric cell and the wall of a heat exchanger of a thermoelectric energy conversion system.

### 5.1. Structural composites

An approach involves taking carbon fiber structural composites as a starting point and modifying these composites for the purpose of enhancing the thermoelectric properties. In this way, the resulting composites are multifunctional (i.e., both structural and thermoelectric). Because structural composites are used in large volumes, the rendering of the thermoelectric function to these materials means the availability of large volumes of thermoelectric materials for use in, say, electrical energy generation. Moreover, temperature sensing is useful for structures for the purpose of thermal control, energy saving and hazard mitigation. The rendering of the thermoelectric function to a structural material also means that the structure can sense its own

temperature without the need for embedded or attached thermometric devices, which suffer from high cost and poor durability. Embedded devices, in particular, cause degradation of the mechanical properties of the structure. The structural composites are specifically cement-matrix composites containing short and randomly oriented fibers, and polymer-matrix composites containing continuous and oriented fibers. In both cases, the fibers serve as the reinforcement.

Two routes are used in the tailoring of the thermoelectric behavior by composite engineering. One route involves the choice of fibers. The other route, which only applies to the polymer-matrix composites, involves the choice of the interlaminar filler, which refers to the particulate filler between the laminae. The former route impacts the thermoelectric properties in any direction for a composite containing randomly oriented fibers. In the case of a composite containing oriented continuous fibers, the former route impacts mainly the thermoelectric properties in the fiber direction of the composite, whereas the latter route impacts mainly the thermoelectric properties in the through-thickness direction of the composite.

#### 5.1.1. Tailoring by choice of fibers

**5.1.1.1. Polymer-matrix composites.** Polymer-matrix composites with continuous oriented carbon fibers are widely used for aircraft, sporting goods and other lightweight structures. Glass fibers and polymer fibers are less expensive than carbon fibers, but they are not conductive electrically and are therefore not suitable for rendering the thermoelectric function to the composite.

Carbon fibers can be *n*-type or *p*-type even without intercalation. Intercalation greatly increases the carrier concentration, thus making the fibers strongly *n*-type or strongly *p*-type, depending on whether the intercalate is an electron donor or an electron acceptor [118]. One of the drawbacks of intercalated graphite is the instability over time, either due to intercalate desorption or reaction with environmental species. For the case of bromine (acceptor) as the intercalate, the instability due to desorption can be overcome by the use of a residue compound, i.e., a compound that has undergone desorption as much as possible so that the remaining intercalate is strongly held, thereby making the compound stable. The stability of bromine intercalated carbon fiber has been demonstrated [119–121]. For the case of an alkali metal such as sodium (donor) as the intercalate, the instability due to reactivity with moisture can be overcome by the use of an alkali metal hydroxide (with the alkali metal ions in excess) as the intercalate [122]. Therefore, the choice of fibers involves using bromine as the acceptor intercalate and sodium hydroxide (with Na<sup>+</sup> ions in excess) as the donor intercalate [123]. By using these dissimilar continuous carbon fibers in adjacent laminae of an epoxy-matrix composite, a thermocouple with sensitivity as high as 82 μV/°C has been attained [123].

The thermocouple junction is the interlaminar interface, as made ordinarily. The junction does not require any bonding agent other than the epoxy, which serves as the matrix of the composite and does not serve as

TABLE II Seebeck coefficient ( $\mu\text{V}/^\circ\text{C}$ ) and absolute thermoelectric power ( $\mu\text{V}/^\circ\text{C}$ ) of carbon fibers and thermocouple sensitivity ( $\mu\text{V}/^\circ\text{C}$ ) of epoxy-matrix composite junctions. All junctions are unidirectional unless specified as crossply. The temperature range is 20–110 $^\circ\text{C}$

	Seebeck coefficient with copper as the reference ( $\mu\text{V}/^\circ\text{C}$ )	Absolute thermoelectric power ( $\mu\text{V}/^\circ\text{C}$ )	Thermocouple sensitivity ( $\mu\text{V}/^\circ\text{C}$ )
P-25 <sup>a</sup>	+0.8	+3.1	
T-300 <sup>a</sup>	-5.0	-2.7	
P-25 <sup>a</sup> + T-300 <sup>a</sup>			+5.5
P-25 <sup>a</sup> + T-300 <sup>a</sup> (crossply)			+5.4
P-100 <sup>a</sup>	-1.7	+0.6	
P-120 <sup>a</sup>	-3.2	-0.9	
P-100 (Na)	-48	-46	
P-100 (Br <sub>2</sub> )	+43	+45	
P-100 (Br <sub>2</sub> ) + P-100 (Na)			+82
P-120 (Na)	-42	-40	
P-120 (Br <sub>2</sub> )	+38	+40	
P-120 (Br <sub>2</sub> ) + P-120 (Na)			+74

<sup>a</sup>Pristine (i.e., not intercalated).

an electrical contact medium (since it is not conducting). In spite of the presence of the epoxy matrix in the junction area, direct contact occurs between a fraction of the fibers of a lamina and a fraction of the fibers of the other lamina, thus resulting in a conduction path in the direction perpendicular to the junction. This conduction path is indicated by direct measurement of the electrical resistance of the junction [124] and enables an electrical contact to be made across the junction. The use of silver paint as an additional bonding agent did not give better result [123]. That a bonding agent did not affect the result is also consistent with the fact that the thermocouple effect is not an interfacial phenomenon. That an additional bonding agent is not necessary facilitates the use of a structural composite as a thermocouple array, as a typical structural composite does not have any extra bonding agent at the interlaminar interface.

Table II shows the Seebeck coefficient and the absolute thermoelectric power of composites and the thermocouple sensitivity of composite junctions. A positive value of the absolute thermoelectric power indicates *p*-type behavior; a negative value indicates *n*-type behavior. Pristine P-25 is slightly *p*-type; pristine T-300 is slightly *n*-type. A junction comprising pristine P-25 and pristine T-300 has a positive thermocouple sensitivity that is close to the difference of the Seebeck coefficients (or the absolute thermoelectric powers) of T-300 and P-25, whether the junction is unidirectional or crossply. Pristine P-100 and pristine P-120 are both nearly zero in the absolute thermoelectric power. Intercalation with sodium causes P-100 and P-120 to become strongly *n*-type. Intercalation with bromine causes P-100 and P-120 to become strongly *p*-type. A junction comprising bromine intercalated P-100 and sodium intercalated P-100 has a positive thermocouple sensitivity that is close to the sum of the magnitudes of the absolute thermoelectric powers of the bromine intercalated P-100 and the sodium intercalated P-100. Similarly, a junction

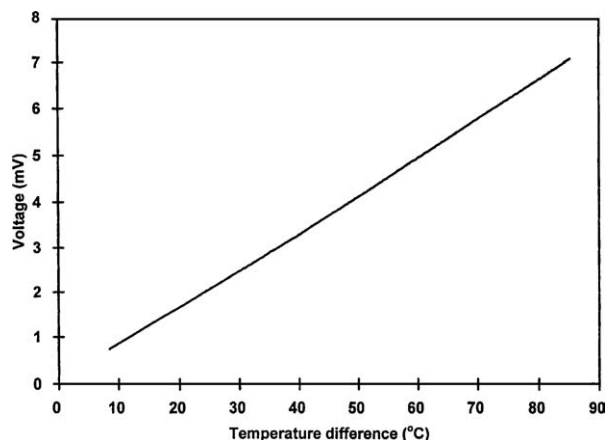


Figure 1 Variation of the measured voltage with the temperature difference between hot and cold points for the epoxy-matrix composite junction comprising bromine intercalated P-100 and sodium intercalated P-100.

tion comprising bromine intercalated P-120 and sodium intercalated P-120 has a positive thermocouple sensitivity that is close to the sum of the magnitudes of the absolute thermoelectric powers of the bromine intercalated P-120 and the sodium intercalated P-120. Fig. 1 shows the linear relationship of the measured voltage with the temperature difference between hot and cold points for the junction comprising bromine intercalated P-100 and sodium intercalated P-100.

5.1.1.2. *Cement-matrix composites.* Cement (Portland cement in this section) is a low-cost, mechanically rugged and electrically conducting materials which can be rendered *n*-type or *p*-type by the use of appropriate admixtures, such as short carbon fibers (which contribute holes) for attaining *p*-type cement and short steel fibers (which contribute electrons) for attaining *n*-type cement (Table III) [125–129]. (Cement itself is weakly *p*-type in relation to electronic/ionic conduction [125]). The fibers also improve the structural properties, such as increasing the flexural strength and toughness and decreasing the drying shrinkage [130–137]. Furthermore, cement-based junctions can be easily made by pouring the dissimilar cement mixes side by side.

Pairs of cement paste were used to make junctions, as described in Table IV [138]. The thermocouple voltage increases monotonically and reversibly with increasing temperature difference for all junctions. The thermocouple voltage noise decreases and the thermocouple sensitivity (Table IV) and reversibility increase in the order: (c), (b) and (a). The highest thermocouple

TABLE III Absolute thermoelectric power ( $\mu\text{V}/^\circ\text{C}$ )

Cement paste	Volume fraction fibers	$\mu\text{V}/^\circ\text{C}$	Type	Ref.
(i) Plain	0	$+2.69 \pm 0.03$	weakly <i>n</i>	[125]
(ii) S <sub>f</sub> (0.5 <sup>a</sup> )	0.10%	$-48.7 \pm 4.8$	strongly <i>n</i>	[129]
(iii) C <sub>f</sub> (0.5 <sup>a</sup> ) + SF	0.48%	$+3.79 \pm 0.09$	weakly <i>n</i>	[125]
(iv) C <sub>f</sub> (1.0 <sup>a</sup> ) + SF	0.95%	$+5.16 \pm 0.11$	<i>p</i>	[125]
(v) C <sub>f</sub> (0.5 <sup>a</sup> ) + L	0.41%	$+3.54 \pm 0.05$	weakly <i>n</i>	[125]

<sup>a</sup>Percentage by mass of cement.

Note: SF = silica fume; L = latex.



TABLE IV Cement junctions

Junction	Pastes involved	Junction type	Thermocouple sensitivity ( $\mu\text{V}/^\circ\text{C}$ )	
			Heating	Cooling
(a)	(iv) and (ii)	<i>pn</i>	$70 \pm 7$	$70 \pm 7$
(b)	(iii) and (ii)	<i>pn</i>	$65 \pm 5$	$65 \pm 6$
(c)	(v) and (ii)	<i>pn</i>	$59 \pm 7$	$58 \pm 5$

Note: *mn*<sup>+</sup> refers to a junction between a weakly *n*-type material and a strongly *n*-type material.

sensitivity is  $70 \pm 7 \mu\text{V}/^\circ\text{C}$ , as attained by junction (a) both during heating and cooling. This value approaches that of commercial thermocouples. That junction (a) gives the best thermocouple behavior (in terms of sensitivity, linearity, reversibility and signal-to-noise ratio) is due to the greatest degree of dissimilarity between the materials that make up the junction. The values of the thermocouple sensitivity (Table IV) are higher than (theoretically equal to) the difference in the absolute thermoelectric power of the corresponding two cement pastes that make up the junction (Table III). For example, for junction (a), the difference in the absolute thermoelectric power of pastes (iv) and (ii) is  $54 \mu\text{V}/^\circ\text{C}$ , but the thermocouple sensitivity is  $70 \mu\text{V}/^\circ\text{C}$ . The reason for this is unclear. Nevertheless, a higher thermocouple sensitivity does correlate with a greater difference in the absolute thermoelectric power.

### 5.1.2. Tailoring by the choice of the interlaminar filler

In contrast to Section 5.1.1, which involves dissimilar fibers to make thermocouples from structural composites, this section uses dissimilar interlaminar fillers for the two thermocouple legs, which have identical fibers. Furthermore, in contrast to Section 5.1.1.1, which exploits the thermoelectric behavior in the fiber direction of a continuous fiber composite, this section exploits the thermoelectric behavior in the through-thickness direction. The use of dissimilar interlaminar fillers is more suitable for practical application than the use of dissimilar fibers, as the method used to obtain sufficiently dissimilar carbon fibers (i.e., intercalation) is expensive and requires highly crystalline carbon fibers, which are also expensive. Glass fibers and polymer fibers are not suitable, as they are not conducting electrically. Steel fibers are conducting, but their high density makes them unsuitable for lightweight composites. As an interlaminar filler has more effect on the properties (particularly the electrical conduction properties) in the through-thickness direction than those in the fiber direction, this section exploits the thermoelectric behavior in the through-thickness direction.

The thermocouple junction (Section 5.1.1.1) that exploits the thermoelectric behavior in the fiber direction involves two dissimilar laminae that form an interlaminar interface, which is the thermocouple junction. The two laminae can be unidirectional or crossply, but the crossply configuration is attractive in that it provides a two-dimensional array of thermocouple junc-

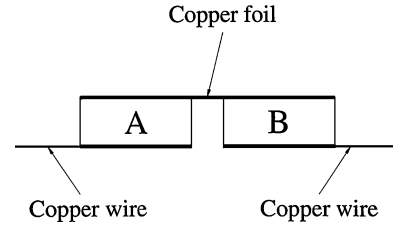


Figure 2 Thermocouple involving dissimilar composites A and B and utilizing the thermoelectric behavior of A and B in the through-thickness direction. In this configuration, the thermocouple junction is exposed.

tions, thereby allowing temperature distribution measurement. Since the thermoelectric behavior in the fiber direction is exploited, only one lamina is needed for each leg. As a consequence, the junction is close to the exposed surface of the laminate and is thus suitable for measuring the temperature of the exposed surface.

On the other hand, for exploiting the thermoelectric behavior in the through-thickness direction, each leg needs to be at least a few laminae in thickness. As a result, the junction is not close to the exposed surface and thus cannot be used to measure the temperature of the exposed surface.

An alternate configuration, as illustrated in Fig. 2, allows the thermocouple junction to be exposed, while each leg comprises multiple laminae. This configuration involves using an electrical interconnection, such as a copper foil that is attached to both laminates. This is the configuration used in this section.

The interlaminar additives used in this section are thermoelectric particles, particularly bismuth, tellurium and bismuth telluride, which are well-known as thermoelectric materials [139]. Table V shows the absolute thermoelectric power obtained in the through-thickness and longitudinal directions for the composites investigated [140]. Even though the sign of the absolute thermoelectric power is different in the directions considered, the addition of the interlaminar thermoelectric particles tends to make it more negative in most cases. The effect is larger in the through-thickness direction than in the longitudinal direction. The thermoelectric behavior of the composite material is influenced by the reinforcing fibers and the interlaminar interfaces. While the fibers govern the behavior in the longitudinal direction, the interlaminar interfaces are encountered in the through-thickness direction. As a result, the effect of the interlaminar particles on the thermal

TABLE V Density, interlayer particle volume fraction and absolute thermoelectric power of various thermoplastic-matrix composites

Set	Density ( $\text{g}/\text{cm}^3$ )	Particle material	Volume fraction particles (%)	Absolute thermoelectric power ( $\mu\text{V}/^\circ\text{C}$ )	
				Through-thickness	Longitudinal
1	$1.4 \pm 0.2$	None	0	$0.5 \pm 0.1$	$-0.7 \pm 0.1$
2	$1.8 \pm 0.2$	Bismuth	$4.5 \pm 0.5$	$0.6 \pm 0.1$	$-0.9 \pm 0.1$
3	$2.3 \pm 0.2$	Bismuth	$10.5 \pm 0.5$	$1.2 \pm 0.1$	$-0.3 \pm 0.1$
4	$1.8 \pm 0.2$	Tellurium	$7.3 \pm 0.5$	$22.3 \pm 0.2$	$-0.1 \pm 0.1$
5	$2.1 \pm 0.2$	Bismuth telluride	$9.9 \pm 0.5$	$-11.7 \pm 1.5$	$-0.8 \pm 0.15$

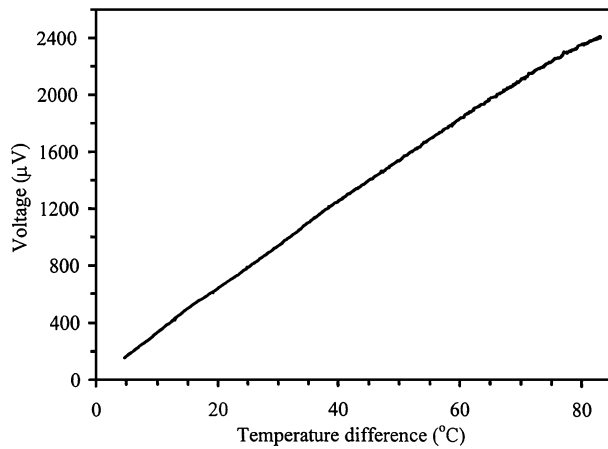


Figure 3 Thermocouple voltage vs. temperature difference for a thermocouple with the configuration of Fig. 2 and involving as the two legs of the thermocouple a composite with tellurium as the interlaminar filler and one with bismuth telluride as the interlaminar filler.

or electrical conduction is expected to be larger in the through-thickness direction than in the longitudinal direction.

The use of tellurium particles is more effective than the use of bismuth particles in making the absolute thermoelectric power more negative, particularly in the through-thickness direction. This is probably because the absolute thermoelectric power is positive for tellurium ( $+70 \mu\text{V}/^\circ\text{C}$  [139]), and this may be favorable for the enhancement of the thermoelectric effect in the composite [141].

In contrast to bismuth ( $-72 \mu\text{V}/^\circ\text{C}$  [133]) and tellurium ( $+70 \mu\text{V}/^\circ\text{C}$  [139]), bismuth telluride ( $+200 \mu\text{V}/^\circ\text{C}$  [139]) makes the absolute thermoelectric power of the composite more negative, particularly in the through-thickness direction. The origin of this effect is unclear.

Because tellurium and bismuth telluride as interlaminar fillers give opposite signs of the absolute thermoelectric power, they were used for making a thermoplastic-matrix composite thermocouple using the configuration of Fig. 2. Fig. 3 [140] shows that the curve of the thermocouple voltage vs. temperature difference is linear. The thermoelectric sensitivity (e.g., thermocouple voltage per unit temperature difference) is  $30 \pm 1.5 \mu\text{V}/^\circ\text{C}$ , which, as expected, is roughly equal to the sum of the magnitudes of the absolute thermoelectric power of the two legs in the through-thickness direction (Table V).

## 5.2. Flexible graphite

The thermal stress between a thermoelectric cell and the wall of a heat exchanger of a thermoelectric energy conversion system affects the thermal coupling as well as the durability. To reduce the thermal stress, compliant pads are used at the interface, although the pad acts as a barrier against thermal conduction [142, 143]. If the thermoelectric material is itself compliant, a compliant pad will not be necessary. Compliant polymer-matrix composites containing a thermoelectric filler suffer from their inability to withstand high temperatures, as encountered in thermoelectric power conver-

sion systems with a high thermal energy density. Flexible graphite is compliant and resistant to high temperatures, in addition to being a thermoelectric material [144].

Metals are in general more compliant than semiconductors, but their Seebeck effect is relatively weak and they tend to suffer from corrosion. Polymers can be more compliant than metals, but they are usually electrically insulating and do not exhibit the Seebeck effect. Flexible graphite is quite unusual in its combination of compliance and thermoelectric behavior.

Flexible graphite is much more conductive thermally in the in-plane direction than in the out-of-plane direction. The high in-plane thermal conductivity, together with the resilience in the out-of-plane direction, help the attaining of a good thermal contact between flexible graphite and a hot/cold surface. On the other hand, the low out-of-plane thermal conductivity is favorable for the Seebeck effect in the out-of-plane direction.

The Seebeck effect in the through-thickness direction of flexible graphite can be used for the generation of electrical energy, as a Seebeck voltage is generated between the two opposite in-plane surfaces of a flexible graphite sheet when the sheet is placed on a hot object (such as a human body) or a cold object (such as the window of an aircraft). The flexibility of the sheet facilitates the placement on a surface which is not flat. A related application is the sensing of the temperature of the hot or cold object.

The absolute thermoelectric power of flexible graphite in the through thickness direction is  $-0.65 \mu\text{V}/^\circ\text{C}$  [145]. For carbons that have not been intercalated, both positive and negative values of the absolute thermoelectric power at room temperature have been reported [144–150]. The value depends on the crystallinity, defects, phonons and impurities, in addition to depending on the carrier type and concentration.

## 6. Sensing

The sensing of strain, damage, temperature, humidity and chemical substances is useful for control and hazard mitigation. Various phenomena can be used to attain sensing. They include electrical and electrochemical phenomena. The electrical phenomena are pertinent to this paper. An electrical phenomenon that enables the sensing of strain is piezoresistivity (i.e., the change of the electrical resistivity with strain or stress). Electrical phenomena that enable the sensing of temperature are the thermistor effect (i.e., the change of the electrical resistivity with temperature) and the Seebeck effect (Section 5). Carbon by itself exhibits weakly piezoresistivity and the thermistor effect [151–153], but carbon fiber composites (with matrices other than carbon), when appropriately designed, exhibit these phenomena strongly. For carbon fiber structural composites, these phenomena enable the composites to be multifunctional. In other words, the structural composites are self-sensing and are thus valuable for smart structures.

Smart structures are structures that have the ability to sense certain stimuli and be able to response to the stimuli in an appropriate fashion, somewhat like a

human being. Sensing is the most fundamental aspect of a smart structure. Smart structures are important due to their relevance to hazard mitigation, structural vibration control, structural health monitoring, transportation engineering, thermal control and energy saving. Research on smart structures has emphasized the incorporation of various devices in a structure for providing sensing, energy dissipation, actuation, control or other functions. Research on smart composites has emphasized the incorporation of a functional material or device in a matrix material for enhancing the smartness or durability. Relatively little attention has been given to the development of structural materials (e.g., concrete and composites) that are inherently able to provide some of the smart functions, so that the need for embedded or attached devices is reduced or eliminated, thereby lowering cost, enhancing durability, increasing the smart volume, and minimizing mechanical property degradation (which usually occurs in the case of embedded devices).

This section is focused on structural composites for smart structures. It addresses cement-matrix and polymer-matrix composites. The smart functions addressed include strain/stress sensing (for structural vibration control, traffic monitoring and weighing), damage sensing (both mechanical and thermal damage in relation to structural health monitoring and hazard mitigation) and temperature sensing (for thermal control, hazard mitigation and structural performance control).

## 6.1. Cement-matrix composites

Cement-matrix composites include concrete (containing coarse and fine aggregates), mortar (containing fine aggregate but no coarse aggregate) and cement paste (containing no aggregate, whether coarse or fine). Other fillers, called admixtures, can be added to the mix to improve the properties of the composite. Admixtures are discontinuous, so that they can be included in the mix. They can be particles, such as silica fume (a fine particulate) and latex (a polymer in the form of a dispersion). They can be short fibers, such as polymer, steel, glass or carbon fibers. They can be liquids such as methylcellulose aqueous solution, water reducing agent, defoamer, etc. Admixtures for rendering the composite smart while maintaining or even improving the structural properties are the focus of this section.

### 6.1.1. Strain sensing

Cement reinforced with short carbon fibers is capable of sensing its own strain due to the effect of strain on the volume electrical resistivity (a phenomenon known as piezoresistivity) [154–171] and due to the effect of strain on the electric polarization (a phenomenon known as direct piezoelectricity) [172].

*6.1.1.1. Piezoresistivity.* Uniaxial tension of carbon fiber reinforced cement in the elastic regime causes reversible increases in the volume electrical resistivity in both longitudinal and transverse directions, such that the gage factor (fractional change in resistance per unit

strain) is comparable in magnitude in the two directions [165]. In contrast, uniaxial compression causes reversible decreases in the resistivity in both directions [166]. Without fibers, the resistivity changes are much smaller and less reversible. The resistivity increase is attributed to defect generation or aggravation under tension and defect healing under compression. The fractional change in resistance per unit strain (i.e., the gage factor) is up to 700.

The transverse resistivity increases upon uniaxial tension, even though the Poisson Effect causes the transverse strain to be negative. This means that the effect of the transverse resistivity increase overshadows the effect of the transverse shrinkage. The resistivity increase is a consequence of the uniaxial tension. In contrast, under uniaxial compression, the resistance in the stress direction decreases. Hence, the effects of uniaxial tension on the transverse resistivity and of uniaxial compression on the longitudinal resistivity are different; the gage factors are negative and positive for these cases respectively.

The similarity of the resistivity change in longitudinal and transverse directions under uniaxial tension suggests similarity for other directions as well. This means that the resistance can be measured in any direction in order to sense the occurrence of tensile loading. Although the gage factor is comparable in both longitudinal and transverse directions, the fractional change in resistance under uniaxial tension is much higher in the longitudinal direction than the transverse direction. Thus, the use of the longitudinal resistance for practical self-sensing is preferred.

Similar piezoresistive behavior has been observed in carbon fiber cement in the form of a coating [167].

*6.1.1.2. Direct piezoelectricity.* The direct piezoelectric effect was observed in cement pastes by voltage measurement [173] and by observing the electric polarization during repeated compressive loading [172]. The piezoelectric effect is attributed mainly to the movement of ions in the cement. The presence of carbon fiber does not enhance the direct piezoelectric effect, though it greatly enhances the piezoresistive effect (Section 6.1.1.1).

### 6.1.2. Damage sensing

Both mechanical damage and thermal damage are of concern to the integrity of cement-based materials. The self-sensing of damage in cement-based materials has been demonstrated with high sensitivity to even minor damage. Work on damage sensing mainly relates to mechanical damage rather than thermal damage, although damage due to freeze-thaw cycling is well-known in cement-based materials, and damage due to heat occurs in fires.

Cement-based materials are capable of sensing major and minor mechanical damage—even damage during elastic deformation—due to the electrical resistivity increase that accompanies damage [174, 175]. The use of short carbon fiber as an admixture enhances the sensitivity [174]. Both damage within the cement-based material and damage at an interface (e.g., the

interface between cement-based materials and steel rebar and that between old and new cement-based materials) can be sensed. Damage within a cement-based material is indicated by increase in the volume electrical resistivity of the material, i.e., the material itself is the sensor [174]. Damage of an interface is indicated by increase in the contact electrical resistivity of the interface [176, 177], i.e., the interface itself is the sensor. That both strain (Section 6.1.1) and damage can be sensed simultaneously through resistance measurement means that the strain/stress condition (during dynamic loading) under which damage occurs can be obtained, thus facilitating damage origin identification. Damage is indicated by a resistance increase which is larger and less reversible when the stress amplitude is higher. The resistance increase can be a sudden increase during loading. It can also be a gradual shift of the baseline resistance.

### 6.1.3. Thermistor

A thermistor is a thermoelectric device consisting of a material (typically a semiconductor, but in this case a cement-based material) whose electrical resistivity changes (typically decreases) with rise in temperature. The carbon fiber cement-based material described in Section 6.1.1 for strain sensing is a thermistor, due to its resistivity decreasing reversibly with increasing temperature [178]; the sensitivity, as indicated by the activation energy (0.4 eV), is comparable to that of semiconductor thermistors. (The effect of temperature will need to be compensated in using the cement-based material as a strain or damage sensor.) Without fibers, the thermistor sensitivity is much lower [178, 179].

## 6.2. Polymer-matrix composites

### 6.2.1. Strain sensing

Self-sensing of strain (reversible) has been achieved in carbon fiber epoxy-matrix composites [180–184], as the electrical resistance of the composite in the through-thickness or longitudinal direction changes reversibly with longitudinal strain (gage factor up to 40) due to change in the degree of fiber alignment. Tension in the fiber direction of the composite increases the degree of fiber alignment, thereby increasing the chance for fibers of adjacent laminae to touch one another. As a consequence, the through-thickness resistance increases while the longitudinal resistance decreases.

The strain sensitivity (gage factor) is defined as the reversible part of  $\Delta R/R_0$  divided by the longitudinal strain amplitude. It is negative (from  $-18$  to  $-12$ ) for the longitudinal  $\Delta R/R_0$  and positive ( $17$ – $24$ ) for the through-thickness  $\Delta R/R_0$ . The magnitudes are comparable for the longitudinal and through-thickness strain sensitivities. As a result, whether the longitudinal  $R$  or the through-thickness  $R$  is preferred for strain sensing just depends on the convenience of electrical contact application for the geometry of the particular smart structure.

A dimensional change without any resistivity change would have caused the longitudinal  $R$  to increase during

tensile loading and decrease during compressive loading. In contrast, the longitudinal  $R$  decreases upon tensile loading and increases upon compressive loading. In particular, the magnitude of  $\Delta R/R_0$  under tension is 7–11 times that of  $\Delta R/R_0$  calculated by assuming that  $\Delta R/R_0$  is only due to dimensional change and not due to any resistivity change. Hence the contribution of  $\Delta R/R_0$  from the dimensional change is negligible compared to that from the resistivity change.

The irreversible behavior, though small compared to the reversible behavior, is such that  $R$  (longitudinal or through-thickness) under tension is irreversibly decreased after the first cycle. This behavior is attributed to the irreversible disturbance to the fiber arrangement at the end of the first cycle, such that the fiber arrangement becomes less neat. A less neat fiber arrangement means more chance for the adjacent fiber layers to touch one another.

### 6.2.2. Damage sensing

Self-sensing of damage (whether due to stress or temperature, under static or dynamic conditions) has been achieved in continuous carbon fiber polymer-matrix composites, as the electrical resistance of the composite changes with damage [185–199]. Minor damage in the form of slight matrix damage and/or disturbance to the fiber arrangement is indicated by the longitudinal and through-thickness resistance decreasing irreversibly due to increase in the number of contacts between fibers. More significant damage in the form of delamination or interlaminar interface degradation is indicated by the through-thickness resistance (or more exactly the contact resistivity of the interlaminar interface) increasing due to decrease in the number of contacts between fibers of different laminae. Major damage in the form of fiber breakage is indicated by the longitudinal resistance increasing irreversibly. During mechanical fatigue, delamination was observed to begin at 30% of the fatigue life, whereas fiber breakage was observed to begin at 50% of the fatigue life [186]. During thermal cycling, damage at the interlaminar interface was indicated by increase of the contact resistivity of the interface [200, 201].

### 6.2.3. Thermistor

Continuous carbon fiber epoxy-matrix composites provide temperature sensing by serving as thermistors [202, 203] and thermocouples (Section 5.1.1.1) [123]. The thermistor function stems from the reversible decrease of the contact electrical resistivity at the interface between fiber layers (laminae) on temperature. From the slope (negative) of the Arrhenius plot, which is quite linear, the activation energy can be calculated. This activation energy is the energy for electron jumping from one lamina to the other. Electronic excitation across this energy enables conduction in the through-thickness direction. The electron jump primarily occurs at points where direct contact occurs between fibers of the adjacent laminae. The direct contact is possible due to the flow of the epoxy resin during composite fabrication and due to the slight waviness of the fibers [185].

### 6.3. Carbon-matrix composites

A carbon-carbon composite with bidirectionally woven continuous carbon fibers has been shown to be an excellent damage sensor, as its electrical resistivity increases irreversibly upon damage, even damage after the first cycle of tensile loading in the elastic regime [204]. However, the strain sensing ability is not as good as that of carbon fiber polymer-matrix composites (Section 6.2.1).

## 7. Electrical switching

Electrical switching can be achieved by using a material whose electrical resistivity increases abruptly under a certain condition (e.g., when the temperature or electric field is above a threshold). The switching serves to protect electronic devices from damage resulting from exceeding the threshold. Polymer-matrix composites containing discontinuous electrically conducting fillers (typically particles) are commonly used for electrical switching. The filler volume fraction is typically in the vicinity of the percolation threshold. The resistivity increases with increasing temperature, due to the large thermal expansion coefficient of the polymer matrix compared to the filler and the consequent decrease in the chance of contact between adjacent filler units as the temperature increases. This phenomenon is known as the positive temperature coefficient (PTC) effect. As the melting temperature or curing temperature of the polymer matrix is approached, the resistivity rises abruptly, thereby providing switching.

Carbon black [205–208], graphite [209], coke [209] and carbon fibers [210] have all been used as discontinuous fillers in polymer-matrix composites for electrical switching. Carbon black is most commonly used, due to its low cost and particulate nature. However, ceramic particles such as  $\text{TiB}_2$  are increasingly used for composites for switching.

## 8. Electronic devices

Electric current rectification (diode behavior) can be achieved by using  $pn$ ,  $nn^+$  or metal-semiconductor junctions. The  $pn$ -junction is the junction between a  $p$ -type conductor (a conductor with holes as the majority carrier) and an  $n$ -type conductor (a conductor with electrons as the majority carrier). The  $pn$ -junction is ideally rectifying, i.e., the current-voltage ( $I$ - $V$ ) characteristic is such that the current is large when the applied voltage is positive on the  $p$ -side relative to the  $n$ -side and is small when the applied voltage is positive on the  $n$ -side relative to the  $p$ -side. The  $pn$ -junction is an electronic device that is central to electrical circuitry, due to its importance to diodes and transistors. Akin to the  $pn$ -junction is the  $n - n^+$  junction, which is a junction between a weakly  $n$ -type conductor and a strongly  $n$ -type (i.e.,  $n^+$ ) conductor.

Electric current rectification and thermocouples (Section 5.1.2) have been attained in cement-based junctions (preferably a  $pn$ -junction, as an  $n - n^+$  junction gives poorer performance), as obtained by separate pouring and co-curing of electrically dissimilar cement mixes side by side [138]. Fig. 4 shows the current-voltage characteristic of a cement-based  $pn$ -junction.

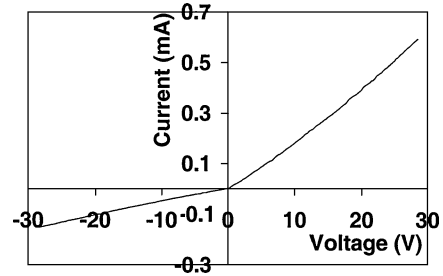


Figure 4 Current-voltage characteristic of a cement-based  $pn$ -junction.

Electric current rectification has also been attained by using junctions between carbon nanotubes, which can be metallic or semiconducting, depending on the chirality [211].

## 9. Thermal pastes

With the miniaturization and increasing power of microelectronics, heat dissipation has become critical to the performance, reliability and further miniaturization of microelectronics. Heat dissipation from microelectronics is most commonly performed by thermal conduction. For this purpose, a heat sink, which is a material of high thermal conductivity, is commonly used. In order for the heat sink to be well utilized, the thermal contact between the heat sink and the heat source (e.g., a substrate with a semiconductor chip on it) should be good [212, 213]. A thermal fluid or paste is commonly applied at the interface to enhance the thermal contact [214]. The fluid or paste is a material that has high conformability so that it can conform to the surface topography of the mating surfaces, thereby avoiding air gaps (which are thermally insulating) at the interface. The fluid or paste must be highly spreadable, so that the thickness of the paste after application is very thin (just enough to fill the valleys in the surface topography of the mating surfaces). Preferably the fluid or paste is thermally conductive as well. Although much attention has been given to the development of heat sink materials, relatively little attention has been given to the development of thermal fluids or pastes.

The most common thermal fluid is mineral oil. As a fluid, it is highly conformable and spreadable, but it has a low thermal conductivity. The most common thermal paste is silicone filled with thermally conductive particles [215–218]. Due to the filler, it is relatively high in thermal conductivity, but it suffers from poor conformability and poor spreadability.

Carbon black dispersions based on polyethylene glycol (PEG) or di(ethylene glycol) butyl ether, along with dissolved ethyl cellulose, provide thermal pastes that are superior to solder as thermal interface materials [219]. The thermal contact conductance of the interface between copper disks reaches  $3 \times 10^5 \text{ W/m}^2 \cdot ^\circ\text{C}$ , compared to  $2 \times 10^5 \text{ W/m}^2 \cdot ^\circ\text{C}$  for a tin-lead-antimony solder. The pastes based on PEG are superior to those based on butyl ether in their thermal stability above  $100^\circ\text{C}$ . Carbon black (of a type that is relatively compressible) is superior to materials that are more conductive thermally (graphite, diamond and nickel particles, carbon filaments and single-walled carbon

TABLE VI Thermal contact conductance for thermal pastes in the form of butyl ether containing 40 vol% ethyl cellulose and 0.27vol% thermally conductive solids, as tested between copper disks at various contact pressures. The interface material was below 25  $\mu\text{m}$  in thickness [219]

Thermally conductive solid	Conductance ( $10^4 \text{ W/m}^2 \cdot ^\circ\text{C}$ )		
	0.46 MPa	0.69 MPa	0.92 MPa
Carbon black	$18.94 \pm 0.60$	$24.87 \pm 1.00$	$25.74 \pm 1.20$
Graphite (5 $\mu\text{m}$ )	$3.03 \pm 0.09$	$3.67 \pm 0.08$	$4.02 \pm 0.12$
Graphite (1 $\mu\text{m}$ )	$1.52 \pm 0.03$	$1.77 \pm 0.04$	$2.04 \pm 0.05$
Nickel (5 $\mu\text{m}$ )	$1.85 \pm 0.05$	$2.14 \pm 0.02$	$2.84 \pm 0.04$
Nickel (1 $\mu\text{m}$ )	$0.91 \pm 0.07$	$2.03 \pm 0.10$	$2.66 \pm 0.03$
Diamond (25 $\mu\text{m}$ )	$1.15 \pm 0.02$	$1.21 \pm 0.09$	$1.54 \pm 0.03$
Carbon filaments (0.1 $\mu\text{m}$ diameter)	$1.09 \pm 0.03$	$1.32 \pm 0.02$	$1.51 \pm 0.03$
Single-walled carbon nanotubes <sup>a</sup>	$13.5 \pm 0.2$	$13.8 \pm 0.3$	$14.1 \pm 0.4$

<sup>a</sup>From Ref. 220.

nanotubes) in providing thermal pastes of high performance (Table VI). The performance of thermal pastes and solder as thermal interface materials is mainly governed by their conformability and spreadability rather than their thermal conductivity.

## 10. Conclusion

The electrical applications of carbons and their composites include electrical conduction (particularly in electrodes, current collectors and electrical contacts), electromagnetic interference shielding, resistance heating, thermoelectric energy conversion, sensing, electrical switching and thermal pastes. They are relevant to the energy, structural, aerospace, electronic and thermal industries.

## References

1. K. KINOSHITA, "Carbon" (Wiley, New York, NY, 1988) p. 405.
2. J. LAHAYE, M. J. WETTERWALD and J. MESSIET, *J. Appl. Electrochem.* **14** (1984) 545.
3. M. DOHZONO, H. KATSUKI and M. EGASHIRA, *J. Electrochem. Soc.* **137** (1989) 1255.
4. D. KOHLER, J. ZABASAJJA, A. KRISHNAGOPALAN and B. TATARCHUK, *ibid.* **137** (1990) 136.
5. J. LAHAYE, M. J. WETTERWALD and J. MESSIER, *J. Appl. Electrochem.* **14** (1984) 117.
6. J. L. WEININGER and C. R. MORELOCK, *J. Electrochem. Soc.* **122** (1975) 116.
7. D. D. L. CHUNG, in "Applications of Submicron Diameter Carbon Filaments," Nanostructured Carbon for Advanced Applications, edited by G. Benedek *et al.* (Kluwer, Netherlands, 2001), p. 331.
8. C. A. FRYSZ, X. SHUI and D. D. L. CHUNG, *J. Power Sources* **58**(1) (1996) 41.
9. L. WEIMING and D. D. L. CHUNG, *Carbon* **40**(ER3) (2002) 447.
10. C. A. FRYSZ, X. SHUI and D. D. L. CHUNG, *J. Power Sources* **58**(1) (1996) 55.
11. *Idem.*, *Carbon* **33**(12) (1995) 1681.
12. S. WILKENING, *Erdol & Kohle Erdgas Petrochemie* **39**(12) (1986) 551.
13. R. PANGRAZZI, W. H. HARTT and R. KESSLER, *Corrosion* **50**(3) (1994) 186.
14. J. HOU and D. D. L. CHUNG, *Cem. Concr. Res.* **27**(5) (1997) 649.
15. G. H. ANDERSON, Cathodic Protection of a Bridge Deck with Silicon Iron Anodes and Coke Breeze Overlay, in Proc. Conf.

- on Cathodic Protection of Reinforced Concrete Bridge Decks. (NACE, Houston, Texas, USA, 1985) p. 82.
16. K. C. CLEAR, in Proc. Conf. on Cathodic Protection of Reinforced Concrete Bridge Decks (NACE, Houston, Texas, USA, 1985) p. 55.
17. J. J. FONTANA and R. P. WEBSTER, *Transp. Res. Rec.* **1041** (1985) 1.
18. V. DUNLAP, Cathodic Protection System Selection, in Proc. Conf. on Cathodic Protection of Reinforced Concrete Bridge Decks (NACE, Houston, Texas, USA, 1985) p. 131.
19. R. F. STRATFULL, Eleven Years of Success for Coke Breeze C. Pavement, in Proc. Conf. on Cathodic Protection of Reinforced Concrete Bridge Decks (NACE, Houston, Texas, USA, 1985) p. 66.
20. W. R. SCHUTT, Cathodic Protection Applied to Bridge Decks, in Proc. Conf. on Cathodic Protection of Reinforced Concrete Bridge Decks (NACE, Houston, Texas, USA, 1985) p. 46.
21. A. A. GADALLAH, A. S. NOURELDIN, F. EZZAT and A. OSMAN, *Transp. Res. Rec.* **968** (1984) 1.
22. M. M. MATEEV and D. L. TOTEV, *Dautschuk & Gummi Kunststoffe* **49**(6) (1996) 427.
23. S. E. ARTEMENKO, L. P. NIKULINA, T. P. USTINOVA, D. N. AKBAROV, E. P. KRAJNOV and V. I. DUBKOVA, *Khimicheskie Volokna* (4) (1992) 39.
24. J. E. TRAVIS, Soc. Plastics Eng. 8th Annual Pacific Technical Conf. and Tech. Displays (Society of Plastics Engineers, Brookfield Center, CT, 1985) p. 98.
25. A. I. MEDALIA, *Rubber Chem. Tech.* **59**(3) (1986) 432.
26. Data Sheet, Controlled Resistivity Alumina for Static Charge Dissipation, WESGO Technical Ceramics, Belmont, CA.
27. A. V. ZEMLYANUKHIN, V. D. ALEKSEEV, T. V. TIMOFEEVA and Y. V. NIKIFIROV, *Steklo i Keramika* (6) (1992) 21.
28. T. M. ZHDANOVA, A. V. ZEMLYANUKHIN and S. N. NEUMEECHEVA, *Glass Ceramics* **48**(3/4) (1991) 168.
29. *Idem.*, *Steklo i Keramika* (4) 1991 24.
30. P. O'SHEA, *Evaluation Eng.* **36**(2) (1997) 6.
31. S. WEN and D. D. L. CHUNG, *J. Electron Mater.* **30**(11) (2001) 1448.
32. P.-W. CHEN and D. D. L. CHUNG, *ACI Mater. J.* **93**(2) (1996) 129.
33. R. BREWER and G. FENICAL, Shielding, *Eval. Eng.* **37**(7) (1998) S4-S10.
34. P. O'SHEA, *Evaluation Eng.* **37**(6) (1998) 40,43,45.
35. S. SHINAGAWA, Y. KUMAGAI and K. URABE, *J. Porous Mater.* **6**(3) (1999) 185.
36. J. HAJDU, *Trans. Inst. Metal. Finishing* **75**(pt. 1) (1997) B7.
37. N. V. MANDICH, *Plat. Surf. Finish.* **81**(10) (1994) 60.
38. C. NAGASAWA, Y. KUMAGAI, K. URABE and S. SHINAGAWA, *J. Porous Mater.* **6**(3) (1999) 247.
39. S. L. THOMPSON, *Evaluation Eng.* **37**(7) (1998) 62,65.
40. D. A. OLIVERO and D. W. RADFORD, *J. Reinf. Plast. Comp.* **17**(8) (1998) 674.
41. K. P. SAU, T. K. CHAKI, A. CHAKRABORTY and D. KHASTGIR, *Plast. Rub. Comp. Proc. Appl.* **26**(7) (1997) 291.
42. C. Y. HUANG and J. F. PAI, *J. Appl. Polym. Sci.* **63**(1) (1997) 115.
43. M. A. SALTZBERG, A. L. NELLER, C. S. HARVEY, T. E. BORNINSKI and R. J. GORDON, *Circuit World* **22**(3) (1996) 67.
44. J. WANG, V. V. VARADAN and V. K. VARADAN, *SAMPE J.* **32**(6) (1996) 18.
45. J. JOO, A. G. MACDIARMID and A. J. EPSTEIN, *Proc. 53rd Annual Tech. Conf.* **2** (1995) 1672.
46. P. YAM, *Sci. Amer.* **273**(1) (1995) 82.
47. H. H. KUHN, A. D. CHILD and W. C. KIMBRELL, *Synthetic Metals* **71**(1-3) (1995) 2139.
48. M. T. NGUYEN and A. F. DIAZ, *Adv. Mater.* **6**(11) (1994) 858.
49. S. H. PENG and K. ZHANG, Finite Element Analysis Aided Engineering of Elastomeric EMI shielding Gaskets, in Proc. 1998 56th Annual Tech. Conf. (Society of Plastic Engineers, Brookfield, CT, 1998) Vol. 2, p. 1216.
50. S. K. DAS, J. NUBEL and B. ZAND, Investigation on the Sources of Shielding Degradation for Gaskets with Zinc Coated

- Steel Enclosures, in Proc. 1997 IEEE 14th International Symposium on Electromagnetic Compatibility (IEEE, Piscataway, NJ, 1997) p. 66.
51. S. H. PENG and W. S. V. TZENG, Recent Developments in Elastomeric EMI Shielding Gasket Design, in Proc. 1997 International Symposium on Electromagnetic Compatibility (IEEE, Piscataway, NJ, 1997) p. 94.
  52. P. O'SHEA, *Eval. Engng.* **36**(8) (1997) 6.
  53. *Idem.*, *ibid.* **35**(8) (1996) 4.
  54. P. B. JANA and A. K. MALLICK, *J. Elast. Plast.* **26**(1) (1996) 58.
  55. L. LI and D. D. L. CHUNG, *Composites* **25**(3) (1994) 215.
  56. X. SHUI and D. D. L. CHUNG, *J. Electron. Mater.* **26**(8) (1997) 928.
  57. X. FU and D. D. L. CHUNG, *Cem. Concr. Res.* **26**(10) (1997) 1467.
  58. J.-M. CHIOU, Q. ZHENG and D. D. L. CHUNG, *Composites* **20**(4) (1989) 379.
  59. X. FU and D. D. L. CHUNG, *Carbon* **36**(4) (1998) 459.
  60. J. CAO and D. D. L. CHUNG, *ibid.* **41**(12) (2003) 2433.
  61. S. WEN and D. D. L. CHUNG, *Cem. Concr. Res.* in press.
  62. [www.achesonindustries.com](http://www.achesonindustries.com)
  63. J. WU and D. D. L. CHUNG, *Carbon* **41**(6) (2003) 1313.
  64. J. CAO and D. D. L. CHUNG, *Cem. Concr. Res.* **33**(11) (2003) 1737.
  65. B. R. CHADHA, D. P. DOBHAL and L. R. GUPTA, *Industr. Lubric. Tribol.* **41**(3) (1989) 4.
  66. M. TSUKUDA, K. TAKADA and K. OZAKI, *Jpn. Inst. Light Metals* **29**(9) (1979) 403.
  67. B. LEE, *Silicone Rubber. Engng.* **236**(10) (1995) 32.
  68. J. C. ROBERTS and P. D. WEINHOLD, *J. Comp. Mater.* **29**(14) (1995) 1834.
  69. M. CHOATE and G. BROADBENT, Toughened Phenolic SMC for EMI Shielding Applications, in Proc. 1996 Regional Tech. Conf. of the Society of Plastic Engineers (Society of Plastics Engineers, Brookfield, CT, 1996) p. 69.
  70. P. D. WIENHOLD, D. S. MEHOKE, J. C. ROBERTS, G. R. SEYLAR and D. L. KIRKBRIDE, Electromagnetic Interference (EMI) Shielding Effectiveness, Surface Resistivity, and RF Conductivity of Thin Composites for Spacecraft Applications, in Proc. 1998 30th International SAMPE Tech. Conf. (SAMPE, Covina, CA, 1998) Vol. 30, p. 243.
  71. A. FERNYHOUGH and Y. YOKOTA, *Comp. IT. Mater. World* **5**(4) (1997) 202.
  72. T. HIRAMOTO, T. TERAUCHI and J. TOMIBE, Controlling ESD and Absorbing and Shielding EMW by Using Conductive Fiber in Aircraft, in Proc. 1998 20th Annual International EOS/ESD Symp. (Electrostatic Discharge Association, Rome, NY, 1998) p. 18.
  73. L. G. MORIN, JR and R. E. DUVALL, Applications for Copper and Nickel-Copper-Nickel Electroplated Carbon Fibers for EMI/RFI Shielding, in Proc. 1998 43rd International SAMPE Symp. and Exhib. (SAMPE, Covina, CA, 1998) Vol. 43, No. 1, p. 874.
  74. J. R. GAIER, M. L. DAVIDSON and R. K. SHIVELY, Durability of Intercalated Graphite Epoxy Composites in Low Earth Orbit, in Proc. 1996 28th International SAMPE Tech. Conf. (SAMPE, Covina, CA, 1996) Vol. 28, p. 1136.
  75. J. M. LIU, S. N. VERNON, A. D. HELLMAN and T. A. CAMPBELL, Electromagnetic Nondestructive Evaluation of Composites for Navy Ship Applications, in Proc. SPIE—The International Society for Optical Engineering (Society of Photo-Optical Instrumentation Engineers, Bellingham, WA, 1995) Vol. 2459, p. 60.
  76. D. A. OLIVERO and D. W. RADFORD, Integrating EMI Shielding into Composite Structure, in Proc. 1996 28th International SAMPE Tech. Conf. (SAMPE, Covina, CA, 1996) Vol. 28, p. 1110.
  77. T. OKABE, K. SAITO, H. TOGAWA and Y. KUMAGAI, *Zairyo/J. Soc. Mater. Sci., Japan* **44**(498) (1995) 288.
  78. L. G. MORIN, JR and R. E. DUVALL, in Proc. 1998 43rd International SAMPE Symp. and Exhib. (SAMPE, Covina, CA, 1998) Vol. 43, No. 1, p. 874.
  79. J. R. GAIER and J. TERRY, in Proc. 1994 7th International SAMPE Electronics Conf. (SAMPE, Covina, CA, 1994) Vol. 7, p. 221.
  80. J. R. GAIER, M. L. DAVIDSON and R. K. SHIVELY, in Proc. 1996 28th International SAMPE Tech. Conf. on Technology Transfer in a Global Community (SAMPE, Covina, CA, 1996) Vol. 28, p. 1136.
  81. J. M. LIU, S. N. VERNON, A. D. HELLMAN and T. A. CAMPBELL, in Proc. of SPIE—The International Soc. for Optical Eng. (Society of Photo-Optical Instrumentation Engineering, Bellingham, WA, 1995) Vol. 2459, p. 60.
  82. D. A. OLIVERO and D. W. RADFORD, in Proc. 1996 28th International SAMPE Tech. Conf. on Technology Transfer in a Global Community (SAMPE, Covina, CA, 1996) Vol. 28, p. 1110.
  83. J. WU and D. D. L. CHUNG, *Carbon* **40**(ER3) (2002) 445.
  84. X. LUO and D. D. L. CHUNG, *ibid.* **34**(10) (1996) 1293.
  85. A. PERKINS and A. GUTHRIE, *Metallurgia* **19**(12) (1982) 605.
  86. K. EBELING, *Betonwerk und Fertigteil—Technik* **60**(12) (1994) 70.
  87. F. LAZZARI and G. RAFFELLINI, *Intern. J. Amb. Energy* **2**(3) (1981) 141.
  88. A. KUMAR, U. SINGH, A. SRIVASTAVA and G. N. TIWARI, *Appl. Energy* **8**(4) (1981) 255.
  89. S. P. SETH, M. S. SODHA and A. K. SETH, *ibid.* **10**(2) (1982) 141.
  90. N. D. KAUSHIK and S. K. RAO, *ibid.* **12**(1) (1982) 21.
  91. A. H. FANNEY, B. P. DOUGHERTY and K. P. DRAMP, Field Performance of Photovoltaic Solar Water Heating Systems, in Proc. 1997 International Solar Energy Conf. (ASME, New York, NY, 1997) p. 171.
  92. K. PELISSIER, T. CHARTIER and J. M. LAURENT, *Ceram. Intern.* **24**(5) (1998) 371.
  93. F. S. G. DOS SANTOS and J. W. SWART, *J. Electrochem. Soc.* **137**(4) (1990) 1252.
  94. M. J. CATTELINO, G. V. MIRAN and B. SMITH, *IEEE Trans. Electr. Dev.* **38**(10) (1991) 2239.
  95. C. C. HUNG, M. E. DILLEHAY and M. STAHL, *J. Aircraft* **24**(10) (1987) 725.
  96. J. XIE, J. WANG, X. WANG and H. WANG, *Hecheng Shuzhi Ji Suliao/Synthetic Resin & Plastics* **13**(1) (1996) 50.
  97. C. SANDBERG, W. WHITNEY, A. NASSAR and G. KUSE, Intelligent Distributed Heater used for Industrial Applications, in Proc. 1995 IEEE International Conf. Systems, Man and Cybernetics (IEEE, Piscataway, NJ 1995) Vol. 4, p. 3346.
  98. V. N. PROKUSHIN, A. A. SHUBIN, V. V. KLEJMENTOV and E. N. MARMER, *Khimicheskie Volkna* (6) (1992) 50.
  99. H. W. LONG and G. E. LONG, Asphaltic Compositions and Uses Therefor, U.S. Patent no. 6,193,793 (2001).
  100. I. V. AVTONOMOV and G. A. PUGACHEV, Resistive Composite Material Based on an Alkaline Slag Binder, *Izvestiya Sibirskogo Otdeleniya Akademii Nauk Sssr, Seriya Tekhnicheskikh Nauk* (1987) Vol. 21, p. 110.
  101. S. YEHIA, C. Y. TUAN, D. FERDON and B. CHEN, *ACI Mater. J.* **97**(2) (2000) 172.
  102. Y. KASAI, *Concr. Int: Design. Constr.* **11**(3) (1989) 33.
  103. W. NAKAGAWA, K. NISHITA and Y. KASAI, Stripping Demolition of Reinforced Concrete by Electric Heating Method, in Proc. 2nd ASME-JSME Nuclear Engineering Joint Conf. (ASME, New York, NY, 1993) p. 871.
  104. F. S. CHUTE, F. E. VERMEULEN and M. R. Cervenán, *Canadian Electr. Eng. J.* **6**(1) (1981) 20.
  105. M. J. CATTELINO, G. V. MIRAN and B. SMITH, *IEEE Trans. Electr. Dev.* **38**(10) (1991) 2239.
  106. C.-C. HUNG, M. E. DILLEHAY and M. STAHL *J. Aircraft* **24**(10) (1987) 725.
  107. J. XIE, J. WANG, X. WANG and HAO WANG, *Hecheng Shuzhi Ji Suliao (Synthetic Resin & Plastics)* **13**(1) (1996) 50.

108. P. L. ZALESKI, D. J. DERWIN and W. H. FLOOD, Jr. Electrically Conductive Paving Mixture and Pavement System, U.S. Patent no. 5,707,171, (1998).
109. P. XIE, P. GU, Y. FU and J. J. BEAUDOIN, Conductive Cement-Based Compositions, U.S. Patent 5,447,564 (1995).
110. P. XIE and J. J. BEAUDOIN, Electrically Conductive Concrete and Its Application in Deicing, ACI SP 154-21, Advances in Concrete Technology, edited by V. M. Malhotra (1995) p. 399.
111. V. N. PROKUSHIN, A. A. SHUBIN, V. V. KLEJMENTOV and EH. N. MARMER, *Khimicheskie Volkna* (6) (1992) 50.
112. B. SONG and R. VISKANTA, *J. Therm. Heat Trans.* **4**(3) (1990) 311.
113. M. HIGAKI, M. NARITA and M. NAKAYAMA, *NEC Research Development* (89) (1988) 81.
114. U.S. Patent No. 5,912,080.
115. U.S. Patent No. 6,083,625.
116. R. CHUGH and D. D. L. CHUNG, *Carbon* **40**(13) (2002) 2285.
117. T. KIM and D. D. L. CHUNG, *ibid.* **41**(12) (2003) 2436.
118. J. TSUKAMOTO, A. TAKAHASHI, J. TANI and T. ISHIGURO, *ibid.* **27**(6) (1989) 919.
119. C.T. HO and D. D. L. CHUNG, *ibid.* **28**(6) (1990) 825.
120. V. GUPTA, R. B. MATHUR, O. P. BAHL, A. MARCHAND and S. FLANDROIS, *ibid.* **33**(11) (1995) 1633.
121. D. E. WESSBERCHER, W. C. FORSMAN and J. R. GAIER, *Synth Met.* **26**(2) (1988) 185.
122. C. HÉROLD, A. HÉROLD and P. LAGRANGE, *J. Phys. Chem. Solids* **57**(6-8) (1996) 655.
123. S. WANG and D. D. L. CHUNG, *Comp. Interf.* **6**(6) (1999) 519.
124. *Idem.*, *ibid.* **6**(6) (1999) 497.
125. S. WEN and D. D. L. CHUNG, *Cem. Concr. Res.* **29**(12) (1999) 1989.
126. M. SUN, Z. LI, Q. MAO and D. SHEN, *ibid.* **28**(4) (1998) 549.
127. *Idem.*, *ibid.* **28**(12) (1998) 1707.
128. *Idem.*, *ibid.* **29**(5) (1999) 769.
129. S. WEN and D. D. L. CHUNG, *ibid.* **30**(4) (2000) 661.
130. P.-W. CHEN and D. D. L. CHUNG, *Composites: Part B* **27B** (1996) 269.
131. *Idem.*, *ACI Mater. J.* **93**(2) (1996) 129.
132. A. M. BRANDT and L. KUCHARSKA, Materials for the New Millennium, in Proc. Mater. Eng. Conf. (ASCE, New York, NY, 1996) Vol. 1, p. 271.
133. N. BANTHIA and J. SHENG, *Cem. Concr. Compos* **18**(4) (1996) 251.
134. B. MOBASHER and C. Y. LI, *ACI Mater. J.* **93**(3) (1996) 284.
135. M. PIGEON, M. AZZABI and R. PLEAU, *Cem. Concr. Res.* **26**(8) (1996) 1163.
136. N. BANTHIA, C. YAN and K. SAKAI, *Cem. Concr. Compos.* **20**(5) (1998) 393.
137. T. URANO, K. MURAKAMI, Y. MITSUI and H. SAKAI, *Composites—Part A: Appl. Sci. Manufact.* **27**(3) (1996) 183.
138. S. WEN and D. D. L. CHUNG, *J. Mater. Res.* **16**(7) (2001) 1989.
139. R. A. HORNE, *J. Appl. Phys.* **30** (1959) 393.
140. V. H. GUERRERO, S. WANG and S. WEN, *J. Mater. Sci.* **37**(19) (2002) 4127.
141. D. J. BERGMAN and L. G. FEL, *J. Appl. Phys.* **85** (1999) 8205.
142. M. KAMBE, *Mater. Sci. Forum* **308-311** (1999) 653.
143. M. ARAI, M. KAMBE, T. OGATA and Y. TAKAHASHI, *Nippon Kikai Gakkai Ronbunshu, a Hen* **62**(594) (1996) 1996.
144. C. UHER, *Phys. Rev. B* **25**(6) (1982) 4167.
145. Y. M. HOI and D. D. L. CHUNG, *Carbon* **40**(7) (2002) 1134.
146. Y. HISHIYAMA and A. ONO, *ibid.* **23**(4) (1985) 445.
147. Y. KABURAGI and Y. HISHIYAMA, *ibid.* **36**(11) (1998) 1671.
148. A. ONO and Y. HISHIYAMA, *Philos. Mag. B—Phys. Cond. Matter. Struct. Electr. Opt. Magn. Prop.* **59**(2) (1989) 271.
149. J. P. HEREMANS, Extended Abstracts and Program—17th Biennial Conference on Carbon (American Carbon Society, University Park, PA, 1985) p. 231.
150. J. TSUKAMOTO, A. TAKAHASHI, T. TANI and T. ISHIGURO, *Carbon* **27**(6) (1989) 919.
151. X. WANG and D. D. L. CHUNG, *ibid.* **35**(5) (1997) 706.
152. S. WANG and D. D. L. CHUNG, *ibid.* **35**(5) (1997) 621.
153. B. T. KELLY, "Physics of Graphite" (Applied Science Publishers, London, 1981).
154. X. FU, W. LU and D. D. L. CHUNG, *Cem. Concr. Res.* **26**(7) (1996) 1007.
155. X. FU, E. MA and D. D. L. CHUNG, *ibid.* **27**(6) (1997) 845.
156. X. FU, W. LU and D. D. L. CHUNG, *ibid.* **28**(2) (1998) 183.
157. P. CHEN and D. D. L. CHUNG, *Smart Mater. Struct.* **2** (1993) 22.
158. *Idem.*, *J. Amer. Ceram. Soc.* **78**(3) (1995) 816.
159. D. D. L. CHUNG, *J. Electroceram.* **6**(1) (2001) 75.
160. P. CHEN and D. D. L. CHUNG, *ACI Mater. J.* **93**(4) (1996) 341.
161. D. D. L. CHUNG, *Smart Mater. Struct.* **4** (1995) 59.
162. X. FU and D. D. L. CHUNG, *Cem. Concr. Res.* **26**(1) (1996) 15.
163. *Idem.*, *ibid.* **27**(9) (1997) 1313.
164. Z. SHI and D. D. L. CHUNG, *ibid.* **29**(3) (1999) 435.
165. S. WEN and D. D. L. CHUNG, *ibid.* **30**(8) (2000) 1289.
166. *Idem.*, *ibid.* **31**(2) (2001) 297.
167. *Idem.*, *ibid.* **31**(4) (2001) 665.
168. Q. MAO, B. ZHAO, D. SHEN, Z. LI, J. WUHAN and U. TECH, *Mater. Sci. Ed.* **11**(3) (1996) 41.
169. Q. MAO, B. ZHAO, D. SHEN and Z. LI, *Fuhe Cailiao Xuebao/Acta Materiae Compositae Sinica* **13**(4) (1996) 8.
170. B. ZHAO, Z. LI, D. WU, J. WUHAN and U. TECH, *Mater. Sci. Ed.* **10**(4) (1995) 52.
171. D. D. L. CHUNG, *J. Mater. Sci.* **36** (2001) 1315.
172. S. WEN and D. D. L. CHUNG, *Cem. Concr. Res.* **31**(2) (2001) 291.
173. M. SUN, Q. LIU, Z. LI and Y. HU, *ibid.* **30**(10) (2000) 1593.
174. D.-M. BONTEA, D. D. L. CHUNG and G. C. LEE, *ibid.* **30**(4) (2000) 651.
175. J. LEE and G. BATSON, Materials for the New Millennium, in Proc. 4th Mater. Eng. Conf. (1996) Vol. 2, p. 887.
176. J. CAO and D. D. L. CHUNG, *Cem. Concr. Res.* **31**(4) (2001) 669.
177. *Idem.*, *J. Mater. Sci.* **36**(18) (2001) 4345.
178. S. WEN and D. D. L. CHUNG, *Cem. Concr. Res.* **29**(6) (1999) 961.
179. W. J. MCCARTER, *J. Amer. Ceram. Soc.* **78**(2) (1995) 411.
180. S. WANG and D. D. L. CHUNG, *Polym. Comp.* **22**(1) (2001) 42.
181. N. MUTO, H. YANAGIDA, T. NAKATSUJI, M. SUGITA, Y. OHTSUKA and Y. ARAI, *Smart Mater. Struct.* **1** (1992) 324.
182. X. WANG, X. FU and D. D. L. CHUNG, *J. Mater. Res.* **14**(3) (1999) 790.
183. X. WANG and D. D. L. CHUNG, *Composites: Part B* **29B**(1) (1998) 63.
184. P. E. IRVING and C. THIOGARAJAN, *Smart Mater. Struct.* **7** (1998) 456.
185. X. WANG and D. D. L. CHUNG, *Polym. Compos.* **18**(6) (1997) 692.
186. X. WANG, S. WANG and D. D. L. CHUNG, *J. Mater. Sci.* **34**(11) (1999) 2703.
187. S. WANG and D. D. L. CHUNG, *Polym. Compos.* **9**(2) (2001) 135.
188. N. MUTO, H. YANAGIDA, M. MIYAYAMA, T. NAKATSUJI, M. SUGITA and Y. OHTSUKA, *J. Ceram. Soc. Jpn.* **100**(4) (1992) 585.



189. N. MUTO, H. YANAGIDA, T. NAKATSUJI, M. SUGITA, Y. OHTSUKA, Y. ARAI and C. SAITO, *Adv. Compos. Mater.* **4**(4) (1995) 297.
190. R. PRABHAKARAN, *Experim. Techn.* **14**(1) (1990) 16.
191. M. SUGITA, H. YANAGIDA and N. MUTO, *Smart Mater. Struct.* **4**(1A) (1995) A52.
192. A. S. KADDOUR, F. A. R. AL-SALEHI, S. T. S. AL-HASSANI and M. J. HINTON, *Comp. Sci. Tech.* **51** (1994) 377.
193. O. CEYSSON, M. SALVIA and L. VINCENT, *Scripta Materialia* **34**(8) (1996) 1273.
194. K. SCHULTE and C. BARON, *Comp. Sci. Tech.* **36** (1989) 63.
195. K. SCHULTE and J. PHYSIQUE IV, *Colloque C7 3* (1993) 1629.
196. J. C. ABRY, S. BOCHARD, A. CHATEAUMINOIS, M. SALVIA and G. GIRAUD, *Comp. Sci. Tech.* **59**(6) (1999) 925.
197. A. TEDOROKI, H. KOBAYASHI and K. MATUURA, *JSME Int. J. Series A—Solid Mech. Streng. Mater.* **38**(4) (1995) 524.
198. S. HAYES, D. BROOKS, T. LIU, S. VICKERS and G. F. FERNANDO, in Proc. SPIE—The Int. Soc. for Optical Engng. **2718** (1996) 376.
199. S. WANG, Z. MEI and D. D. L. CHUNG, *Int. J. Adh. Adh.* **21**(ER6) (2001) 465.
200. S. WANG and D. D. L. CHUNG, *Polym. Polym. Comp.* **9**(2) (2001) 135.
201. S. WANG, Z. MEI and D. D. L. CHUNG, *Int. J. Adh. Adh.* **21**(ER6) (2001) 465.
202. S. WANG and D. D. L. CHUNG, *Comp. Interf.* **6**(6) (1999) 497.
203. *Idem.*, *Composites: Part B* **30**(6) (1999) 591.
204. *Idem.*, *Carbon* **35**(5) (1997) 621.
205. P. J. MATHER and K. M. THOMAS, *J. Mater. Sci.* **32**(7) (1997) 1711.
206. H. TANG, X. CHEN and Y. LUO, *Eur. Polym. J.* **32**(8) (1996) 963.
207. C.-M. CHAN, C.-L. CHENG and M. M. F. YUEN, *Polym. Eng. Sci.* **37**(7) (1997) 1127.
208. M. OMASTOVÁ, J. PROKEŠ, S. PODHRADSKÁ and I. CHODÁK, *Macromol. Symp.* **170** (2001) 231.
209. N. A. KOVALENKO and I. K. SYROVATSKAYA, *Int. Polym. Sci. Tech.* **28**(6) (2001) T/57.
210. Y. CHEKANOV, R. OHNOGI, S. ASAI and M. SUMITA, *J. Mater. Sci.* **34**(22) (1999) 5589.
211. Z. YAO, H. W. C. POSTMA, L. BALENTS and C. DEKKER, *Nature* **402** (1999) 273.
212. E. G. WOLFF and D. A. SCHNEIDER, *Int. J. Heat Mass Transfer* **41**(22) (1998) 3469.
213. T. OUELLETTE and M. DE SORGO, Thermal Performance of Heat Transfer Interface Materials, in Proc. Power Electronics Design Cont., Power Sources Users Conf. (Cerritos, CA, 1985) p. 134.
214. M. R. VOGEL, Thermal Performance for a Miniature Heat Sink Cooled by MicroPCM Slurry, in Proc. Int. Intersociety Electronic Packaging Conf., Adv. In Electronic Packaging (American Society of Mechanical Engineers, New York, NY, 1995) Vol. 10–12, p. 989.
215. S. W. WILSON, A. W. NORRIS, E. B. SCOTT and M. R. COSTELLO, Thermally Conductive Adhesives for Highly Thermally Stressed Assembly, National Electronic Packaging and Production Conf., Proc. Technical Program (Reed Exhibition Companies, Norwalk, CT, 1996) Vol. 2, p. 788.
216. A. L. PETERSON, Silicones with Improved Thermal Conductivity for Thermal Management in Electronic Packaging, in Proc. 40th Electronic Components and Tech. Conf. (IEEE, Piscataway, NJ, 1990) Vol. 1, p. 613.
217. X. LU, G. XU, P. G. HOFSTRA and R. C. BAJCAR, *J. Polym. Sci., Part B* **36**(13) (1998) 2259.
218. T. SASASKI, K. HISANO, T. SAKAMOTO, S. MONMA, Y. FIJMORI, H. IWASAKI and M. ISHIZUKA, Development of sheet type thermal conductive compound using AlN. Japan IEMP Symp. Proc., IEEE/CPMT Int. Electronic Manufacturing Technology (IEMT) Symp. (IEEE, Piscataway, NJ, 1995) p. 236.
219. C.-K. LEONG and D. D. L. CHUNG, *Carbon* **41**(13) (2003) 2459.
220. Y. XU, C. K. LEONG and D. D. L. CHUNG, unpublished results.

Received 14 July  
and accepted 29 October 2003